NEDD8-activating enzyme inhibition activates c-Myc-mediated apoptotic pathway in cancer cells

（NEDD8 活性化酵素阻害は、がん細胞において c-Myc を介し apoptosis 経路を活性化し抗がん作用を発揮する）

千葉大学大学院医学薬学府
先端医学薬学専攻
（主任：田中知明　教授）
GUZHANUER AILIKEN

ABSTRACT

c-Myc signaling and its upstream regulators, such as FUBP1-interacting repressor and BRG1 pathway, have been shown to be drug targets for various cancers. On the other hand, neddylation is the process by which the molecule NEDD8 is attached to cellular proteins. Recently proposed post-translational modification that is involved in many diseases including cancer. TAS4464 is an effective selective small molecule inhibitor of NEDD8 activating enzyme (NAE), this leads to inactivation of cullin-Ring E3 ubiquitin ligase (CRLs) and the accumulation of substrate proteins. Here, I investigated the antitumor properties and mechanism of action of TAS4464 on cancer cell lines. TAS4464 induced cell growth stagnation and cell death in different AML cell lines regardless of their genetic background. In AML cells, TAS4464 activates caspase-9 and caspase-8, which are involved in intrinsic and extrinsic apoptotic pathways. I found that TAS4464 induced the activation of pro-apoptotic factor NOXA in apoptotic pathway with changes at the mRNA transcriptional level. RNA sequencing analysis showed that, the CRL substrate c-Myc signaling pathway was involved in the regulation mechanism by TAS4464 treatment. A chromatin immunoprecipitation (ChIP) assay showed that TAS4464-induced c-Myc bound to promoter region of *PMAIP1*(encoding NOXA), accompanied by modification changes in both active and inhibitory histone markers. Moreover, TAS4464 accumulates c-Myc in MCF7 breast cancer cells, similar to AML cell lines. The knock out of c-Myc neutralized the anti-tumor effect by TAS4464 partially in MCF7 cells. These findings suggest that NAE inhibition leads to anti-cancer activity with a novel c-Myc-dependent apoptosis induction.

Introduction

Neddylation is one of the post-transcriptional modifications of NEDD8 binding to substrate proteins [1]. NEDD8 is a ubiquitin-like protein that can change the conformation of its target substrate. Neddylation is believed to control many biological processes such as cell proliferation, senescence and apoptosis [2-6]. The conjugation of NEDD8 to its substrates were catalyzed by NEDD8 activating enzyme E1 (NAE: a heterodimer comprising APPBP1 and UBA3 subunits) and NEDD8-conjugating enzyme E2 (Ubc12/UBE2M or UBE2F) [7, 8]. The most obvious substrate for ubiquitin modification is the cullin family of proteins, which are the core scaffold components of cullin-Ring E3 ligase (CRLs) [9, 10]. The CRLs are the largest ubiquitin E3 ligase family and is known to be activated by neddylation. Activated CRLs promote ubiquitin binding to substrate proteins, which are degraded by the ubiquitin-proteasome system [11]. Currently, number of studies had reported that neddylation is associated with tumor growth and survival [12-14]. Hence, the inhibition of ubiquitin-like pathway by targeting NAE is considered as a novel therapeutic strategy for malignancy. In fact, MLN4924/TAK-924 (Pevonedistat), one of NAE inhibitors, has been developed as anti-tumor agent clinically [15-19].

Recently, it is reported that new NAE inhibitor TAS4464, which is the most potent and selective NAE inhibitor, showed extensive anti-proliferative activity against various cancer cell lines. TAS4464 also showed wide therapeutic effect due to its long-acting NAE inhibition in tumors and low off-target effect. Here, I had extensively studied the role of TAS4464 in tumor cells and found that TAS4464 activated apoptosis pathways. TAS4464 activates caspase activities via enhancing NOXA. This molecule is

transcriptionally regulated by c-Myc as direct target. The anti-tumor mechanism mediated by TAS4464 may explain how NAE inhibition will be applied for the patients as a novel therapeutic reagent.

Materials and Methods

Cell lines and cell cultures

OCI-AML2, SKM-1 and SHI-1 were obtained from German Collection of Microorganisms and Cell Cultures (DMSZ). NOMO-1 was obtained from Health Science Research Resources Bank (HSRRB). Kasumi-1, HL-60, KG-1, MV4-11 and THP-1 were obtained from American Type Culture Collection (ATCC). KG-1a was obtained from European Collection of Authenticated Cell Cultures (ECCAC). All cell lines were cultured in the recommended media and serum concentrations, according to the instructions accompanying the cell lines. All cell lines were reauthenticated by means of short tandem repeat–based DNA profiling.

Chemical Compounds and antibodies

TAS4464 was designed and synthetized at Taiho Pharmaceutical Co., Ltd. and Cytarabine (Cytosine beta-D-arabinofuranoside hydrochloride) was purchased from SIGMA-ALDRICH Co. LLC. Anti-cleaved caspase-3 (#9664), anti-cleaved caspase-8 (#9496), anti-cleaved caspase-9 (#9501) and anti-Bcl2l10 (#3869) were purchased from Cell Signaling Technology, Inc. anti-c-Myc (sc-40) and anti-β-actin (sc-1615) antibodies were purchased from Santa Cruz Biotechnology, Inc. anti-NEDD8 (ab81264), anti-NOXA (ab13654), anti-c-Myc (ab32072) and anti-α-Tubulin (ab4047) were purchased from Abcam plc.

Cell viability assay

Cancer cells were plated in a 96-well plate and incubated overnight. For cell viability assay, TAS4464 was added, followed by incubation for 3 days. Cell viability was evaluated using CellTiter-Glo (Promega Corp.).

Apoptosis analysis

Cells were treated with TAS4464 for the indicated times. For apoptosis analysis, the harvested cells were stained a FITC Annexin V Apoptosis Detection Kit I (BD Pharmingen ^{TM}) for HL-60 cells or with an Annexin V -633 Apoptosis Detection Kit^{TM} (nacalai tesque^{TM}) for MCF7 cells according to the manufacturer's protocol. In brief, 1×10^5 cells were incubated with 5μl of Annexin V and 5μl of propidium iodide (PI) at room temperature in the dark. The cells were analyzed immediately by flow cytometry [FACSCanto^{TM}II, (BD Biosciences)].

Immunoblot analysis

Cells were lysed in lysis buffer [M-PER Mammalian Protein Extraction Reagent (Thermo Fisher Scientific Inc.) supplemented with cOmplete, Mini, Protease Inhibitor Cocktail (Roche Applied Science) and PhosSTOP Phosphatase Inhibitor Cocktail (Roche Applied Science)]. Proteins were separated by SDS-PAGE and transferred to polyvinylidene fluoride membranes (Bio-Rad Laboratories, Inc.). Membranes were blocked with Blocking One blocking reagent (Nacalai Tesque, Inc.) and probed with the appropriate primary antibodies. The membranes were then incubated with horseradish peroxidase–linked secondary antibodies (Cell Signaling Technology, Inc.), and proteins were visualized by means of luminol-based enhanced chemiluminescence (Thermo

Fisher Scientific Inc.). Luminescent images were captured with a LAS-4000 imaging system (Fuji Photo Film Co., Ltd.) or Amersham Imager 600 (GE Healthcare

Generation of knockout cell lines

The protocol used for the CRISPR/Cas9 system was consistent with that reported by Cong et al [20]. The backbone vector pX458 pSpCas9(BB)-2A-GFP was obtained from Addgene. The target guide RNA sequences were designed at the *MYC* (5'-CTATGACCTCGACTACGACT-3'). These oligos were annealed and phosphorylated using T4 DNA Ligase Reaction Buffer and T4 Polynucleotide Kinase (New England Biolabs) at 37℃ for 30 min and 95℃ for 5 min. pX458 was digested using BbsI (Thermo Fisher Scientific Inc.) at 37℃ for 30 min and purified using a QIAquick Gel Extraction Kit (QIAGEN). The ligation reaction of pX458 and the annealed oligos was performed at room temperature for 10 min using a Quick Ligation Kit (New England Biolabs). Then, the ligated reactants were purified using PlasmidSafe exonuclease (Cambio) at 37℃ for 30 min. The plasmids were transformed into Stbl3, and amplified plasmids were purified using NucleoBond Xtra Midi (Takara). Each plasmid was transfected into MCF7 using Lipofectamine 2000 (Thermo Fisher Scientific Inc.) according to the manufacturer's protocol. The plasmid-expressing MCF7 were selected by GFP soating using BD FACS Aria III ether to establish the monoclonal cell lines.

Quantitative reverse-transcribed polymerase chain reaction (RT-PCR)

PMAIP1 (encoding NOXA) primer (ID: Hs00560402_m1) and 18S rRNA primer (ID: Hs99999901_s1) were purchased from Thermo Fisher Scientific Inc. Cells were treated with TAS4464 for the times indicated. After the cells were harvested, total RNAs were isolated with RNeasy Plus Mini Kit (QIAGEN) and were subsequently reverse-

transcribed into cDNA with SuperScript™ III RT (Thermo Fisher Scientific Inc.). Solutions for qRT-PCR were prepared with TaqMan® Gene Expression Assays (Thermo Fisher Scientific Inc.) following the supplier's protocol. qRT-PCR was performed using QuantStudio™ 7 Flex System (Thermo Fisher Scientific Inc.) with default setting of Fast mode (stage 1; 95.0 °C for 20 sec, stage 2; 95.0 °C for 1 sec and 60.0 °C for 20 sec with 40 repeats).

RNA-sequence analysis and non-target proteomics analysis

HL-60 cells were either not treated (control) or treated with TAS4464 (0.1 μmol L^{-1}) for 24 or 48 hours. Then, RNA was isolated from the cell samples using a phenol-guanidinium isothiocyanate (P/GTC) reagent according to the manufacturer's protocol [21]. RNA was precipitated from the aqueous phase with isopropanol, and proteins were precipitated from the phenol/ethanol phase by the addition of acetone. A total of single-end-read RNA-seq tags were generated using a HiSeq 2000 sequencer according to the standard protocol. The generated sequence tags were mapped onto the human genome sequence (hg19 from the University of California Santa Cruz Genome Browser) using the Eland program (Illumina). RNA-seq data are available in the National Bioscience Database Center database (http://humandbs.biosciencedbc.jp/)(accession no. xxxxxx). The protein extract was digested, and the peptides were analyzed by LC-MS/MS (Q Exactive Orbitrap HF-X). Differential expression was estimated and analyzed with the TCC software package in R/Bioconductor 3.1 for each library with reference to the control. The mass spectrometry proteomics data have been deposited in the ProteomeXchange Consortium (http://proteomecentral.proteomexchange.org) via the jPOST partner repository (http://jpostdb.org) with the dataset identifier PXD021012/ JPST000944.

Chromatin Immunoprecipitation (ChIP)

HL-60 cells (1×10^6) were seeded and were fixed 2 days later with 0.5% formaldehyde in IMDM for 10 min at 37 °C. The reaction was quenched by the addition of 700 µl of 2.5M glycine, and the cells were washed with PBS. Pelleted nuclei were dissolved in lysis buffer [50 mM Tris-HCl (pH 8.0), 1% SDS and 10 mM EDTA] and sonicated in a UD-201ultrasonic disruptor (Tomy) with 50 cycles of sonication for 5 sec followed by rest for 5 sec at the power specified in programmed memory setting 4. Ten micrograms of an anti-c-Myc antibody mixture [a mixture of anti-c-Myc (SC-40) and anti-c-Myc (ab32072)] was separately prebound to Dynabeads Protein A/G (Invitrogen) and then added individually to the diluted chromatin complexes in parallel aliquots. The samples were incubated overnight at 4 °C, washed, and eluted for 6 hours at 65°C in ChIP elution buffer [40m M Tris-HCl (pH 6.5), 0.1M NaHCO3, 1% SDS, 0.2 M NaCl, 10 mM EDTA and 10 µg μl^{-1} proteinase K]. Precipitated chromatin fragments were cleaned using a PCR purification kit (Qiagen). The samples were analyzed by qPCR at the region sites in the *PMAIP1* and *CFLAR* promoters. The primer sequences used are listed in Supplemental Table 1.

Statistical analysis

Statistical significance of the differences in numerical data was assessed with a Student's t-test and ANOVA with Tukey's test or Dunnett's test (Xenograft model). All tests were two-tailed and a P-value below 0.05 was considered significant. All data analyses were performed using Microsoft Excel version 14.6.2 (Microsoft Corporation, Redmond, Washington), GraphPad Prism version 8.4.3 and R software (www.r-project.org/).

Results

TAS4464 induces apoptosis in AML cell lines regardless of their genetic background

Antiproliferative activity of TAS4464 in 10 AML cell lines was evaluated. Although each AML cell line tested harbors various types of genetic abnormalities translocations, TAS4464 treatments resulted in decrease in cell viability in all evaluated AML cell lines with GI_{50} values of 0.0003 to 1 μmol L^{-1} (Figure 1A). Suggesting that TAS4464 induced apoptosis in AML cell lines independent of their genetic background. Then, we confirmed by Annexin V staining that the apoptotic cell death was induced by TAS4464 treatment in HL-60 cells (Figure 1B).

There are two well-characterized apoptosis cascades such as the intrinsic and the extrinsic apoptotic pathways, and several caspases play critical roles as initiator or effector caspases in each apoptotic pathway. To assess the involvement of these apoptotic pathways in TAS4464-induced cell death, activities of caspases were evaluated upon treatment with TAS4464 in AML cells. TAS4464 treatment resulted in activation of caspase-8 and caspase-9 among initiator caspases, and all known effector caspases such as caspase-3 (Figure 1C).

TAS4464 increases *PMAIP1* mRNA transcriptional level

To examine which apoptotic factors upstream caspase-8 and caspase-9 are involved in TAS4464-mediated apoptosis, changes in the Bcl-2 family proteins and the death receptor signal-related proteins were evaluated upon treatment with TAS4464. Inhibition of neddylation pathway by TAS4464 was observed as decrease in the amount of NEDD8-conjugated form of Ubc12 and cullin1 (Figure 2A).

Subsequently NOXA was specifically upregulated among Bcl-2 family proteins time-dependently in HL-60 and THP-1 cells (Figure 2B). To further pursue the mechanisms leading to upregulation of NOXA, we confirmed that *PMAIP1* mRNA (gene name of NOXA) was upregulated time-dependently up to 24 hours upon treatment with TAS4464 (Figure 2C). These data suggest that NOXA is regulated at both of protein and transcriptional level by TAS4464 treatment.

TAS4464 treatment activates c-Myc pathway by escaping protein degradation

RNA sequencing analysis revealed the gene expression of HL-60 cells treated with DMSO or TAS4464. The whole expression pattern changed after treatment, and the longer exposure time led to more significant difference (Figure 3A). To assess the continuous effect of TAS4464, we focused the genes which were sustainably affected up to 48h. As a result, we identified 1106 upregulated genes and 3623 downregulated genes by comparison between two groups at two time points (24h and 48h) (Figure 3B and 3C). Pathway analysis based on commonly affected genes revealed that cancer-related pathways such as DNA damage response and breast cancer signaling were highly involved in TAS4464 treatment. (Figure 3D). We then predicted the upstream regulators for altered genes using Upstream Regulator Analysis tool and found the candidates including *MYC* and *TP53* (Figure 3D). Among them, c-Myc signaling was considered to be the most relevant pathway in apoptosis induction on AML because c-Myc is one of the transcription factors regulated by CRLs, and it has been reported that *MYC* has roles for positive regulation of *PMAIP1*. It is also one of the reasons for focusing c-Myc signaling that HL-60 is p53-null cell line, and furthermore, there have been no report on

the association between apoptotic induction and HNF4a in AML. Therefore, we investigated the correlation between c-Myc and NOXA in AML cells.

In fact, the differentially expressed genes contained many *MYC*-related genes in the gene clusters affected by TAS4464 , (Figure 3E). In addition, qRT-PCR was used to verify the actual gene expression level of the upregulated cluster treated with TAS4464. (Figure 3F)

TAS4464-induced c-Myc directly regulates *PMAIP1* gene expression by binding to its gene promoter

Because c-Myc functions as a transcriptional factor, I focused on c-Myc protein level through the time course up to 24h after TAS4464 induction. As a result, the c-Myc protein level made a peak at 4 to 8 hours after treatment (Figure 4A and Figure 4B). Proteomics analysis in HL-60 cells showed the differentially expressed *MYC* target molecules each time point with TAS4464 treatment (Figure 4C). *MYC*-dependent molecules were differentially expressed in the affected by TAS4464.

MYC-dependent *PMAIP1* expression could be sometimes regulated by MYC recruitment at non-consensus sequence sites [22, 23]. Therefore, ChIP-qPCR assay was performed upon treatment with TAS4464 (0.1 μmol L^{-1}) for 4 hours in HL-60 cell. Primer pairs were designed for targeting the consensus c-Myc binding sequence within the promoter regions of *PMAIP1* (Figure 4D). I found that c-Myc proteins were enriched approximately 200 bp upstream of the transcription start site (TSS) in HL-60 cells. c-Myc binding at this location was observed even in steady state, but it was significantly increased by TAS4464 induction (Figure 4D). Taken together, I conclude that TAS4464 treatment enhance *PMAIP1* transcription by recruiting c-Myc direct binding.

Contribution of c-Myc to TAS4464-induced MCF7 cell death.

TAS4464 has previously been reported to inhibit cell growth in a variety of malignancies [24], but its effectiveness varies by cell type. Therefore, I investigated the mechanism of action of the above mechanisms on the occurrence and development of solid tumors. c-Myc accumulation resulted from TAS4464 treatment in MCF7 (breast cancer) cells, similar to AML cell lines (Figure 5A), and c-Myc knockout (c-Myc KO) decreased TAS4464-mediated molecular responses, such as NOXA induction and Caspase cleavage (Figure 5B). Consistently, c-Myc KO inhibited the cell death, even though the basal survival rate was higher in control cells (Figure 5C). This suggests that the molecular effects of TAS4464 may vary depending on cell type or culture conditions.

Discussion

Protein neddylation is a recently proposed post-translational modification that is involved in many diseases including cancer [25]. Inhibition of neddylation pathway has been expected to inhibit tumor growth in patients. In this study, I demonstrated the molecular mechanism of novel NAE inhibitor, TAS4464, for human AML regression.

Among hypothesized mechanisms of NAE inhibition for AML, I found that TAS4464 increased in NOXA in several AML cell lines. Synergistically, these molecules could inhibit the tumor growth through apoptotic pathways [26, 27]. In fact, comprehensive analysis showed that the *MYC* pathway was highly correlated with the molecules affected by TAS4464 treatment. c-Myc is widely accepted to be a protooncogene since its activation has been observed more than 70% of total cancers and played roles to initiate oncogenic process and cell proliferation. The transcriptional activity of c-Myc is mainly regulated by the dimerization with Max, and the dysregulation of the dimerization has been proposed the therapeutic target for cancers [28]. On the other hand, overexpression of c-Myc leads to apoptotic response independent of Max recruitment. For instance, c-Myc is responsible for cell death in Burkitt's lymphoma cells deprived of autocrine factors. Epithelial cells have also been shown to be susceptible to apoptosis by c-Myc. In addition, c-Myc is required to respond effectively to a variety of apoptotic stimuli including transcription and translation inhibitors, hypoxia, heat shock, DNA damage and cancer chemotherapy [29]. The cells with high expression of c-Myc activate p53 and change the metabolic status [30]. In addition, recent studies have shown that NAE inhibition induces c-Myc accumulation followed by NOXA induction [31]. In this study, I found that c-Myc regulated NOXA at its transcription level. These pathways induce

apoptosis in AML cell line, thus their transactivation by c-Myc may provide beneficial effect for cancer therapy.

However, the antitumor effect of TAS4464 through apoptosis may not be fully explained by c-Myc regulation alone. First, cultured tumor cells exhibited c-Myc activation, but the time range was limited in the initial few hours. Second, c-Myc inhibition could not completely reverse the expression of NOXA to the basic levels, while TAS4464 still remains the anti-tumor activity under c-Myc inhibition (data not shown). Third, c-Myc bound to the promoter regions of *PMAIP1* in response to TAS4464. However, c-Myc regulated the target genes partially for certain, therefore uncovered mechanism such as p53 pathway or HNF4A pathway could function in an accommodating way based on my result. Further research is needed to clarify their combination.

In conclusion, I presented the activation of apoptotic pathway by TAS4464 in AML cells. This regulation is mediated by NOXA and leads to the activation of caspase activity. TAS4464 is now been evaluating under Phase I clinical trial in patients with tumors. This study provides important evidence for TAS4464 as an anti-tumor agent.

Acknowledgments

Thank you for Masataka Yokoyama, Kazuyuki Yamagata, Hidekazu Nagano, Akitoshi Nakayama, Naoko Hashimoto, Kazutaka Murata, Motoi Nishimura, Yusuke Kawashima, Osamu Ohara and Tomoaki Tanaka are affiliated with Chiba University. Hiroaki Ochiiwa, Chihoko Yoshimura, Hiromi Muraoka, Keiji Ishida and Shuichi Ohkubo are full-time employees of Taiho Pharmaceutical Co., Ltd. Chihoko Yoshimura and Shuichi Ohkubo have ownership interest in a patent WO2015199136.

References

1. Gong L, Yeh ET. Identification of the activating and conjugating enzymes of the NEDD8 conjugation pathway. J Biol Chem 1999; 274: 12036-12042.

2. Petroski MD, Deshaies RJ. Function and regulation of cullin-RING ubiquitin ligases. Nat Rev Mol Cell Biol 2005; 6: 9-20.

3. Soucy TA, Smith PG, Rolfe M. Targeting NEDD8-activated cullin-RING ligases for the treatment of cancer. Clin Cancer Res 2009; 15: 3912-3916.

4. Pan Y, Xu H, Liu R, Jia L. Induction of cell senescence by targeting to Cullin-RING Ligases (CRLs) for effective cancer therapy. Int J Biochem Mol Biol 2012; 3: 273-281.

5. Read MA, Brownell JE, Gladysheva TB, Hottelet M, Parent LA, Coggins MB et al. Nedd8 modification of cul-1 activates SCF(beta(TrCP))-dependent ubiquitination of IkappaBalpha. Mol Cell Biol 2000; 20: 2326-2333.

6. Barkett M, Gilmore TD. Control of apoptosis by Rel/NF-kappaB transcription factors. Oncogene 1999; 18: 6910-6924.

7. Kamitani T, Kito K, Nguyen HP, Yeh ET. Characterization of NEDD8, a developmentally down-regulated ubiquitin-like protein. J Biol Chem 1997; 272: 28557-28562.

8. Enchev RI, Schulman BA, Peter M. Protein neddylation: beyond cullin-RING ligases. Nat Rev Mol Cell Biol 2015; 16: 30-44.

9. Hori T, Osaka F, Chiba T, Miyamoto C, Okabayashi K, Shimbara N et al. Covalent modification of all members of human cullin family proteins by NEDD8. Oncogene 1999; 18: 6829-6834.

10. Pan ZQ, Kentsis A, Dias DC, Yamoah K, Wu K. Nedd8 on cullin: building an expressway to protein destruction. Oncogene 2004; 23: 1985-1997.

11. Soucy TA, Dick LR, Smith PG, Milhollen MA, Brownell JE. The NEDD8 Conjugation Pathway and Its Relevance in Cancer Biology and Therapy. Genes Cancer 2010; 1: 708-716.

12. Xie P, Zhang M, He S, Lu K, Chen Y, Xing G et al. The covalent modifier Nedd8 is critical for the activation of Smurf1 ubiquitin ligase in tumorigenesis. Nat Commun 2014; 5: 3733.

13. Li L, Wang M, Yu G, Chen P, Li H, Wei D et al. Overactivated neddylation pathway as a therapeutic target in lung cancer. J Natl Cancer Inst 2014; 106: dju083.

14. Xie P, Yang JP, Cao Y, Peng LX, Zheng LS, Sun R et al. Promoting tumorigenesis in nasopharyngeal carcinoma, NEDD8 serves as a potential theranostic target. Cell Death Dis 2017; 8: e2834.

15. Swords RT, Erba HP, DeAngelo DJ, Bixby DL, Altman JK, Maris M et al. Pevonedistat (MLN4924), a First-in-Class NEDD8-activating enzyme inhibitor, in patients with acute myeloid leukaemia and myelodysplastic syndromes: a phase 1 study. Br J Haematol 2015; 169: 534-543.

16. Shah JJ, Jakubowiak AJ, O'Connor OA, Orlowski RZ, Harvey RD, Smith MR et al. Phase I Study of the Novel Investigational NEDD8-Activating Enzyme Inhibitor Pevonedistat (MLN4924) in Patients with Relapsed/Refractory Multiple Myeloma or Lymphoma. Clin Cancer Res 2016; 22: 34-43.

17. Sarantopoulos J, Shapiro GI, Cohen RB, Clark JW, Kauh JS, Weiss GJ et al. Phase I Study of the Investigational NEDD8-Activating Enzyme Inhibitor Pevonedistat (TAK-924/MLN4924) in Patients with Advanced Solid Tumors. Clin Cancer Res 2016; 22: 847-857.

18. Bhatia S, Pavlick AC, Boasberg P, Thompson JA, Mulligan G, Pickard MD et al. A phase I study of the investigational NEDD8-activating enzyme inhibitor pevonedistat (TAK-924/MLN4924) in patients with metastatic melanoma. Invest New Drugs 2016; 34: 439-449.

19. Lockhart AC, Bauer TM, Aggarwal C, Lee CB, Harvey RD, Cohen RB et al. Phase Ib study of pevonedistat, a NEDD8-activating enzyme inhibitor, in combination with docetaxel, carboplatin and paclitaxel, or gemcitabine, in patients with advanced solid tumors. Invest New Drugs 2019; 37: 87-97.

20. Cong L, Ran FA, Cox D, Lin S, Barretto R, Habib N *et al*. Multiplex genome engineering using CRISPR/Cas systems. *Science* 2013; 339: 819-823.

21. Kawashima Y, Miyata J, Watanabe T, Shioya J, Arita M, Ohara O. Proteogenomic Analyses of Cellular Lysates Using a Phenol-Guanidinium Thiocyanate Reagent. *J Proteome Res* 2019; 18: 301-308.

22. Wirth M, Stojanovic N, Christian J, Paul MC, Stauber RH, Schmid RM *et al*. MYC and EGR1 synergize to trigger tumor cell death by controlling NOXA and BIM transcription upon treatment with the proteasome inhibitor bortezomib. *Nucleic Acids Res* 2014; 42: 10433-10447.

23. Ricci MS, Jin Z, Dews M, Yu D, Thomas-Tikhonenko A, Dicker DT *et al*. Direct repression of FLIP expression by c-myc is a major determinant of TRAIL sensitivity. *Mol Cell Biol* 2004; 24: 8541-8555.

24. Yoshimura C, Muraoka H, Ochiiwa H, Tsuji S, Hashimoto A, Kazuno H *et al*. TAS4464, A Highly Potent and Selective Inhibitor of NEDD8-Activating Enzyme, Suppresses Neddylation and Shows Antitumor Activity in Diverse Cancer Models. *Mol Cancer Ther* 2019; 18: 1205-1216.

25. Zhou L, Jiang Y, Luo Q, Li L, Jia L. Neddylation: a novel modulator of the tumor microenvironment. *Mol Cancer* 2019; 18: 77.

26. Bogenberger J, Whatcott C, Hansen N, Delman D, Shi CX, Kim W *et al*. Combined venetoclax and alvocidib in acute myeloid leukemia. *Oncotarget* 2017; 8: 107206-107222.

27. Conti S, Petrungaro S, Marini ES, Masciarelli S, Tomaipitinca L, Filippini A *et al*. A novel role of c-FLIP protein in regulation of ER stress response. *Cell Signal* 2016; 28: 1262-1269.

28. Chen H, Liu H, Qing G. Targeting oncogenic Myc as a strategy for cancer treatment. *Signal Transduct Target Ther* 2018; 3: 5.

29. Hoffman B, Liebermann DA. Apoptotic signaling by c-MYC. *Oncogene* 2008; 27: 6462-6472.

30. Phesse TJ, Myant KB, Cole AM, Ridgway RA, Pearson H, Muncan V *et al*. Endogenous c-Myc is essential for p53-induced apoptosis in response to DNA damage in vivo. *Cell Death Differ* 2014; 21: 956-966.

31. Knorr KL, Schneider PA, Meng XW, Dai H, Smith BD, Hess AD *et al*. MLN4924 induces Noxa upregulation in acute myelogenous leukemia and synergizes with Bcl-2 inhibitors. *Cell Death Differ* 2015; 22: 2133-2142.

Figure legends

Figure 1. TAS4464 induces apoptosis in AML cell lines.

(a) AML cell lines were seeded on 96-well plates and treated the next day with variable concentrations of TAS4464. After 3 days, viable cells were determined by measurement of cellular ATP contents. (b) Apoptotic cell death was evaluated by flow cytometric analysis. HL-60 cells were treated with TAS4464 (0.1 μmol L^{-1}) for 24 hours. (c) THP-1 and HL-60 cells were treated with TAS4464 (0.1 μmol L^{-1}) for 1, 4, 8, 16 and 24 hours and the proteins were extracted. Active form of each caspase was detected by immunoblot with the indicated antibodies.

Figure 2. TAS4464 increases NOXA with changes at the mRNA transcriptional level

(a) THP-1 and HL-60 cells were treated with TAS4464 (0.1 μmol L^{-1}) for 1, 4, 8, 16 and 24 hours and the proteins were extracted. Immunoblot for Bcl-2 family proteins involved in intrinsic apoptotic pathway and death receptor signal-related proteins involved in extrinsic apoptotic pathway were performed with the indicated antibodies. (b) qRT-PCR of *PMAIP1* mRNA were performed in TAS4464 (0.1 μmol L^{-1}) -treated cells relative to control sample. 18S rRNA expression was used to normalize *PMAIP1* mRNA expression. Data are presented as mean ± SD values of data from three independent experiments. * $P < 0.05$, ** $P < 0.01$, *** $P < 0.001$, **** $P < 0.0001$.

Figure 3. RNA-seq results for TAS4464-treated HL-60 cells.

(a) Principal component analysis showing the clusters of HL-60 cells depending on the duration of TAS4464 treatment. DMSO (control) was used for the untreated condition. (b) RNA-seq data for each population. Differentially expressed mRNAs are listed using hierarchical clustering. The top 30 upregulated genes in TAS4464-treated HL-60 cells were listed. (c) 1106 upregulated genes and 3623 downregulated genes by comparison between

two groups at two time points (24h and 48h). (d) Upstream regulators were predicted using Ingenuity Pathway Analysis based on the difference in gene expression between untreated cells and cells treated with TAS4464(0.1 μmol L^{-1})-treated HL-60 cells for 24 hours. (e) Volcano plot data plotted the gene expression changed between untreated and TAS4464 (0.1 μmol L-1)-treated HL-60 cells for 24 hours. Difference of TAS4464-treated cells in m-value was compared to untreated cells. Among MYC-related genes, some larger of mvalue and -log10 (pvalue) genes were labeled. (f) qRT-PCR was performed to compare the mRNA levels of *CDKN1A, TNF* and *E2F1* in cells treated with TAS4464 (0.1 μmol L^{-1}) and control cells. 18S rRNA expression was used for normalization and data are presented as the mean ± SD values of data from three independent experiments. * $P < 0.05$, ** $P < 0.01$, *** $P < 0.001$, **** $P < 0.0001$.

Figure 4. TAS4464 increases the protein stability of c-Myc.

(a) Immunoblotting for c-Myc in HL-60 cells treated with TAS4464 (0.1 μmol L^{-1}). Samples were harvested at 1, 4, 8, 16 and 24 hours after treatment. (b) Changes in c-Myc protein expression levels identified in proteomic analysis during treatment with TAS4464 (0.1 μmol L^{-1}) for up to 24 hours. Data are presented as the mean ± SD values of data from three independent experiments. (c) Proteomics analysis data for each population. Differentially expressed mRNAs are listed using hierarchical clustering. Representative c-Myc target genes are shown in the list. (d) Schematic representation of the *PMAIP1* promoter region. Primer sets are indicated as BS1 to BS5 in *PMAIP1* ChIP assays in *PMAIP1* promoter region were performed with anti-c-Myc antibody, in HL-60 cells after treatment with DMSO or TAS4464 (0.1 μmol L^{-1}) for 4 hours.

Figure 5. c-Myc knockout by CRISPR-Cas9 genome editing in MCF7 cells.

(a) c-Myc was knocked out by the CRISPR-Cas9 system in MCF7 cells. (b) Immunoblotting for c-Myc, NOXA, Cleaved caspase-8 and Cleaved caspase-9 was performed in unedited or c-Myc KO MCF7 cells treated with or without TAS4464 (0.1 μmol L^{-1}) for 36 hours. (c) MCF7 cells were treated with TAS4464 (0.1 μmol L^{-1}) for 36 hours. Apoptotic cells analyzed immediately by flow cytometry.

Figure 1

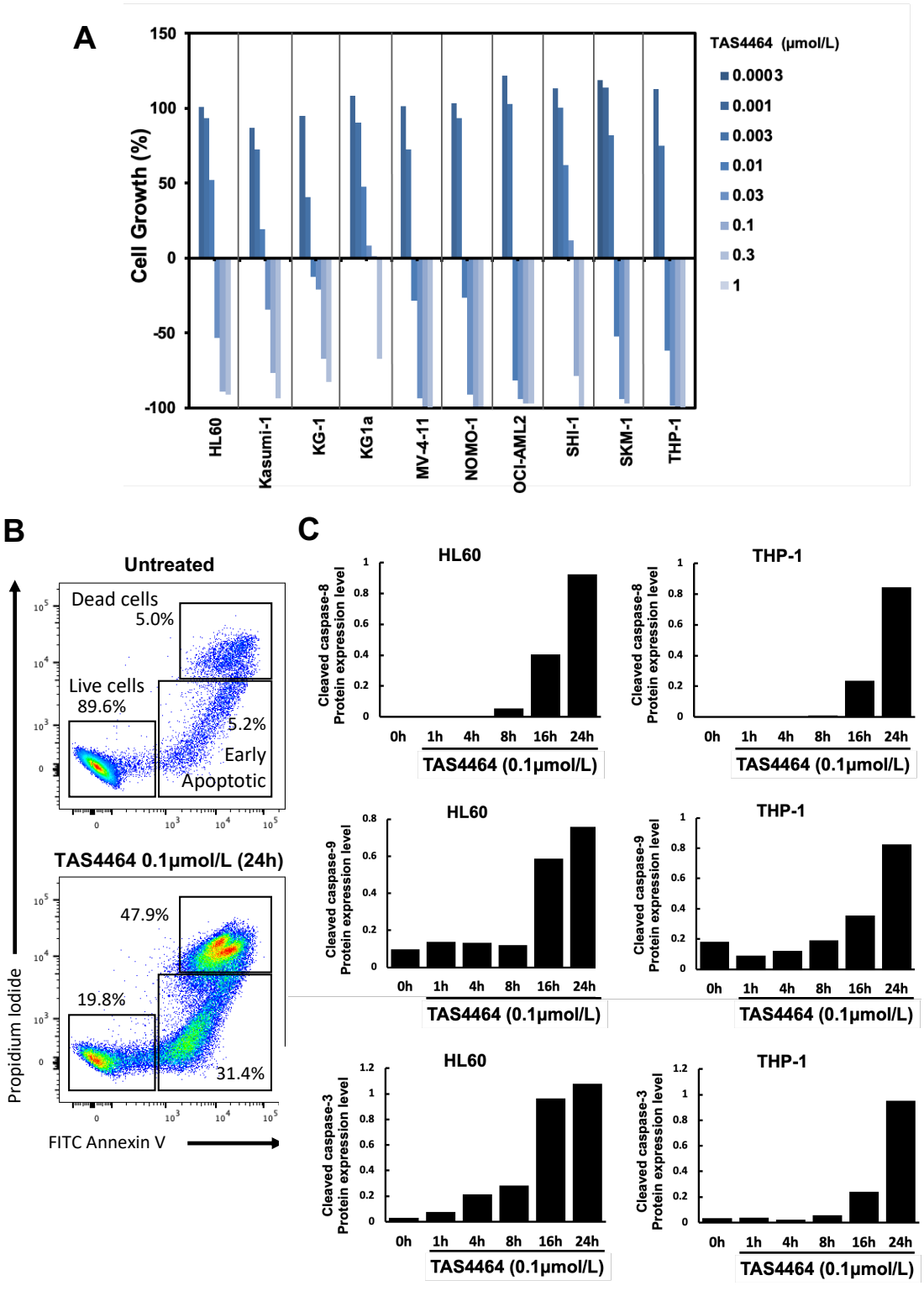
A
Cell Growth (%)
150
100
50
0
-50
-100
HL60
Kasumi-1
KG-1
KG1a
MV-4-11
NOMO-1
OCI-AML2
SHI-1
SKM-1
THP-1
TAS4464 (μmol/L)
0.0003
0.001
0.003
0.01
0.03
0.1
0.3
1
B
Untreated
Dead cells
5.0%
Live cells
89.6%
5.2%
Early
Apoptotic
TAS4464 0.1μmol/L (24h)
47.9%
19.8%
31.4%
Propidium Iodide
FITC Annexin V
C
HL60
THP-1
Cleaved caspase-8 Protein expression level
Cleaved caspase-9 Protein expression level
Cleaved caspase-3 Protein expression level
0h
1h
4h
8h
16h
24h
TAS4464 (0.1μmol/L)

Figure 2

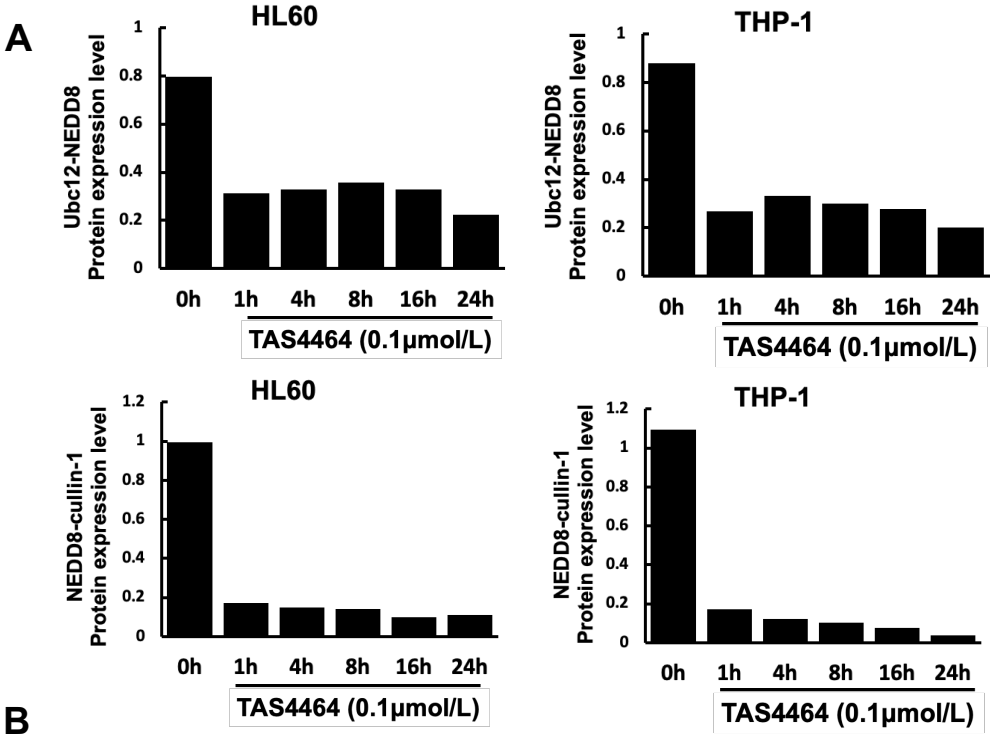
A
HL60
THP-1
Ubc12-NEDD8
Protein expression level
NEDD8-cullin-1
Protein expression level
0h 1h 4h 8h 16h 24h
TAS4464 (0.1μmol/L)

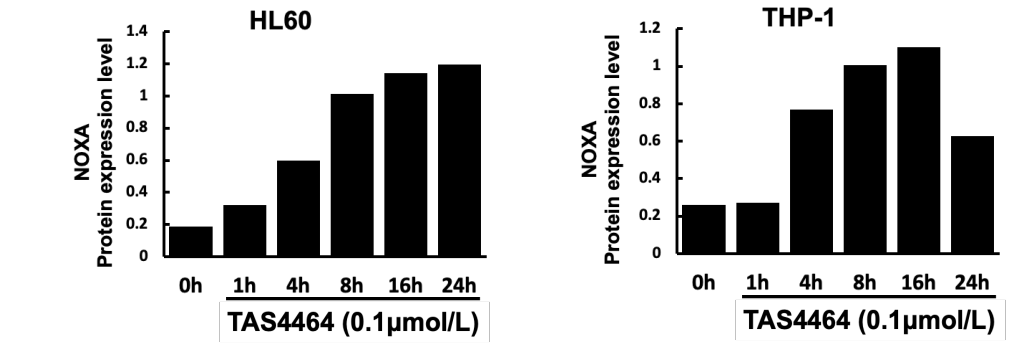
B
HL60
THP-1
NOXA
Protein expression level
0h 1h 4h 8h 16h 24h
TAS4464 (0.1μmol/L)

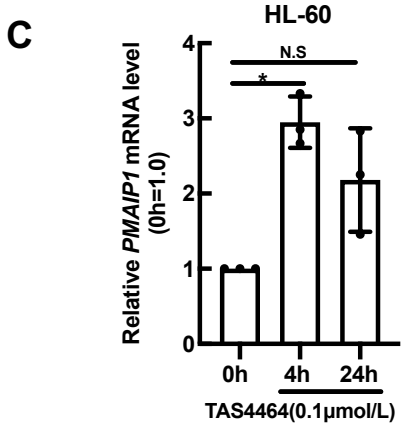
C
HL-60
THP-1
Relative PMAIP1 mRNA level
(0h=1.0)
N.S
*
0h 4h 24h
TAS4464(0.1μmol/L)

Figure 3

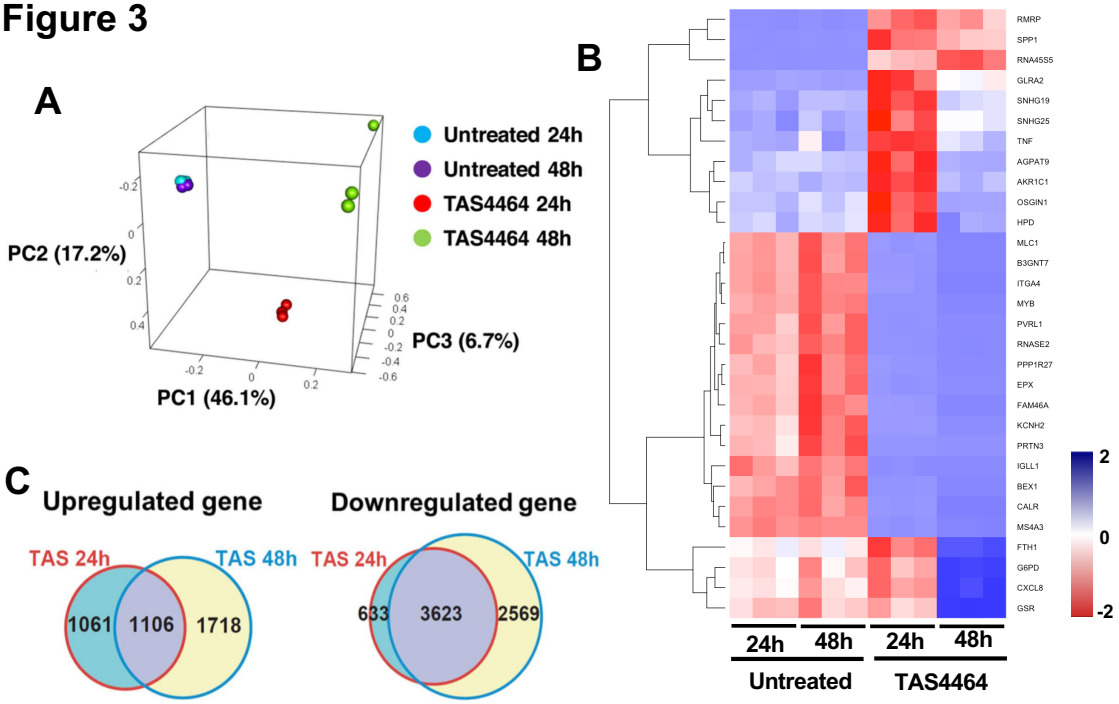

D

Pathways	p-value
EIF2 Signaling	3.23E-26
Role of BRCA1 in DNA Damage Response	2.09E-12
Hereditary Breast Cancer Signaling	1.39E-10
tRNA Charging	1.92E-10
Mitochondrial Dysfunction	2.74E-10

Upstream Regulators	p-value
HNF4A	1.84E-47
MYC	9.56E-37
TP53	1.38E-34
CD 437	4.83E-28
ST1926	1.12E-25

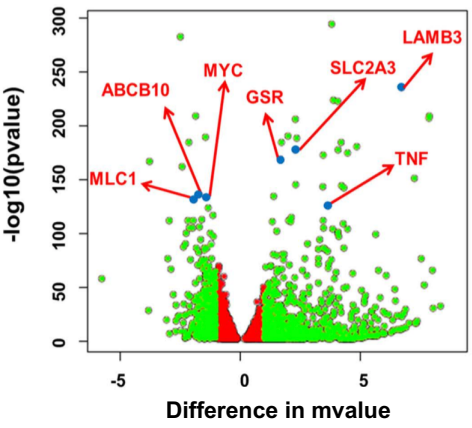

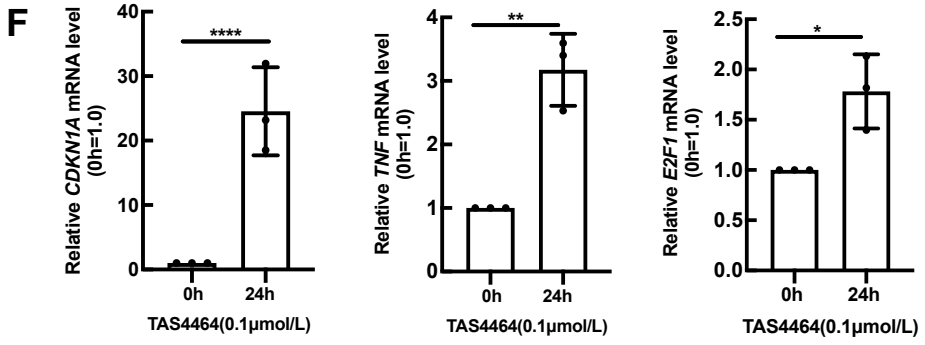

Figure 4

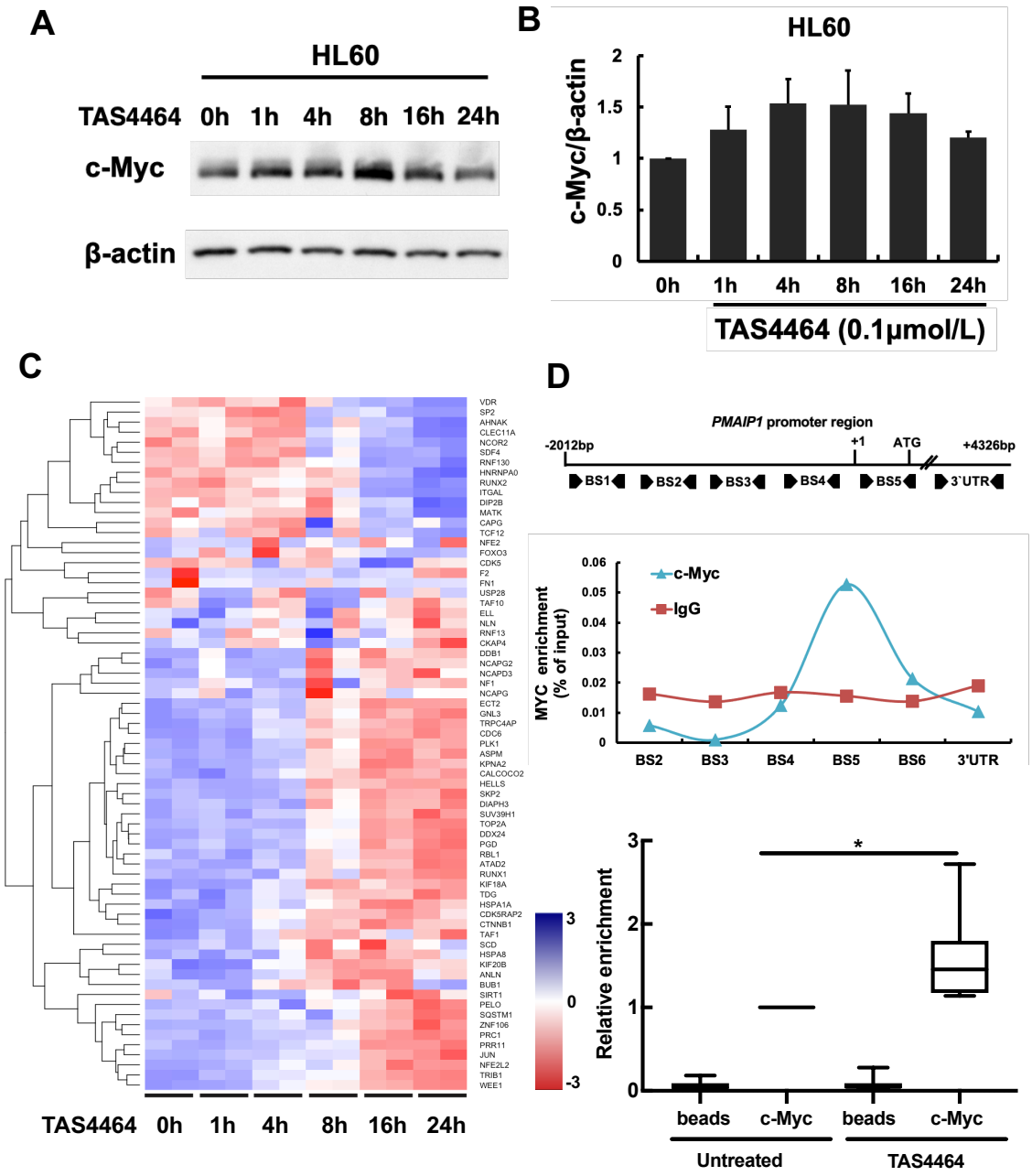
A
HL60
TAS4464 0h 1h 4h 8h 16h 24h
c-Myc
β-actin
B
HL60
c-Myc/β-actin
2
1.5
1
0.5
0
0h 1h 4h 8h 16h 24h
TAS4464 (0.1μmol/L)
C
VDR
SP2
AHNAK
CLEC11A
NCOR2
SDF4
RNF130
HNRNPA0
RUNX2
ITGAL
DIP2B
MATK
CAPG
TCF12
NFE2
FOXO3
CDK6
F2
FN1
USP28
TAF10
ELL
NLN
RNF13
CKAP4
DDB1
NCAPG2
NCAPD3
NF1
NCAPG
ECT2
GNL3
TRPC4AP
CDC6
PLK1
ASPM
KPNA2
CALCOCO2
HELLS
SKP2
DIAPH3
SUV39H1
TOP2A
DDX24
PGD
RBL1
ATAD2
RUNX1
KIF18A
TDG
HSPA1A
CDK5RAP2
CTNNB1
TAF1
SCD
HSPA8
KIF20B
ANLN
BUB1
SIRT1
PELO
SQSTM1
ZNF106
PRC1
PRR11
JUN
NFE2L2
TRIB1
WEE1
TAS4464 0h 1h 4h 8h 16h 24h
3
0
-3
D
PMAIP1 promoter region
-2012bp
+1
ATG
+4326bp
BS1 BS2 BS3 BS4 BS5 3`UTR
c-Myc
IgG
MYC enrichment (% of input)
0.06
0.05
0.04
0.03
0.02
0.01
0
BS2 BS3 BS4 BS5 BS6 3'UTR
Relative enrichment
3
2
1
0
*
beads c-Myc beads c-Myc
Untreated
TAS4464

Figure 5

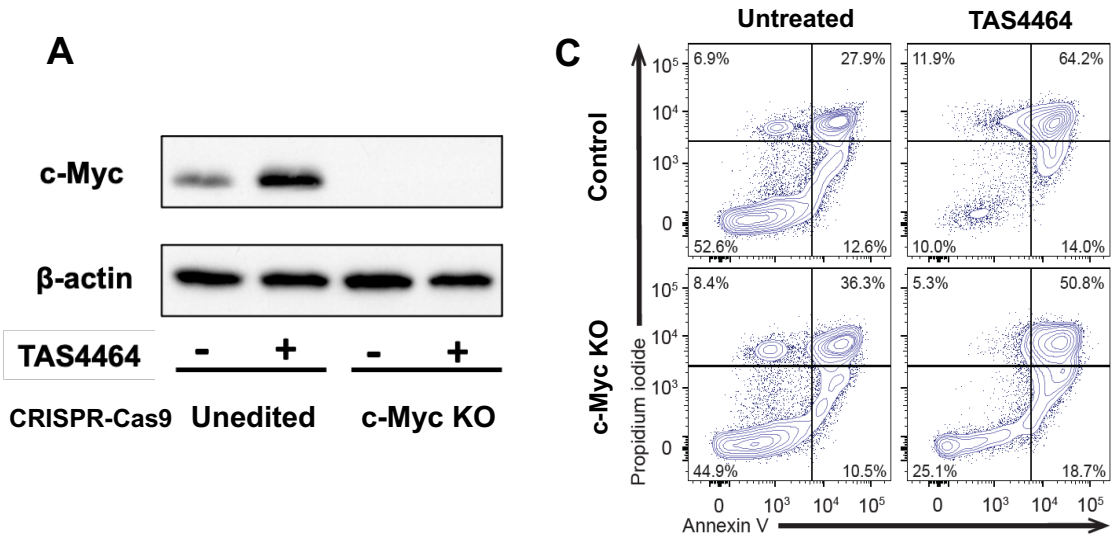
A
c-Myc
β-actin
TAS4464 - + - +
CRISPR-Cas9 Unedited c-Myc KO
C
Untreated
TAS4464
Control
c-Myc KO
6.9%
27.9%
52.6%
12.6%
11.9%
64.2%
10.0%
14.0%
8.4%
36.3%
44.9%
10.5%
5.3%
50.8%
25.1%
18.7%
Propidium iodide
Annexin V

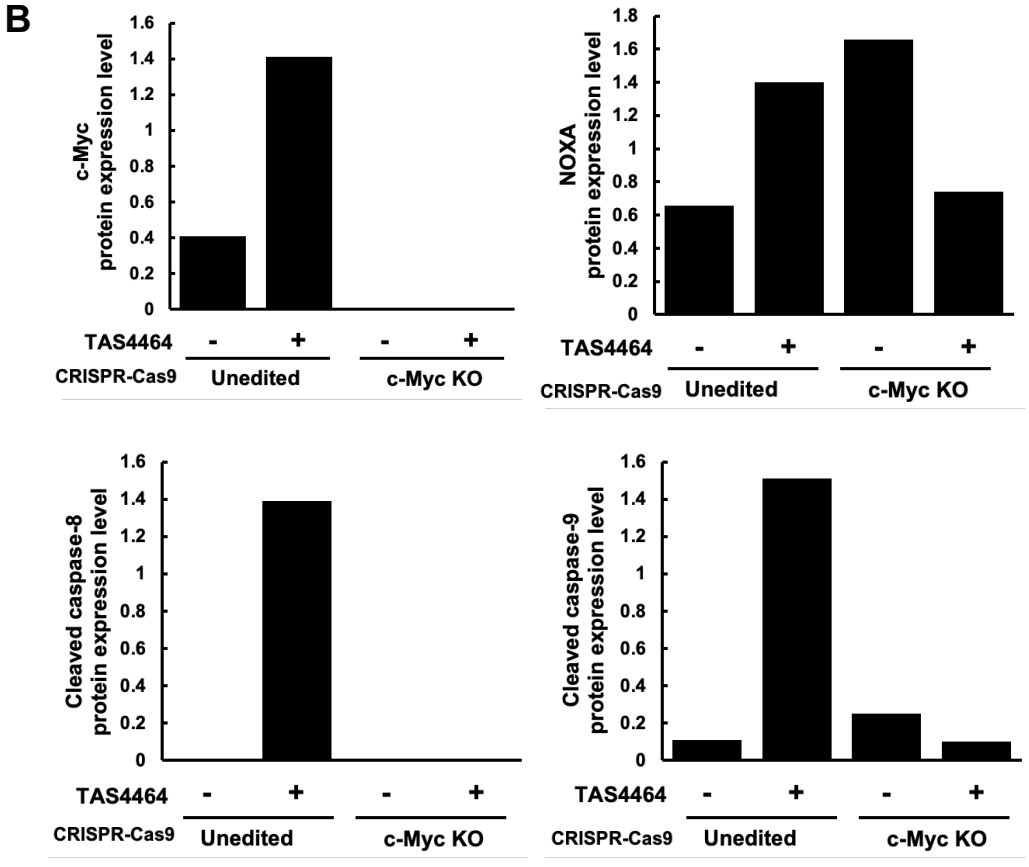
B
c-Myc protein expression level
NOXA protein expression level
Cleaved caspase-8 protein expression level
Cleaved caspase-9 protein expression level
TAS4464 - + - +
CRISPR-Cas9 Unedited c-Myc KO

Supplementary Table 1 ChIP primer sequences

The listed primers were used for ChIP-qPCR to detect c-Myc binding.

Supplemental Table 1	
Gene name	**Sequence**
PMAIP1_BS1_Forward	CTTCGACCACACTTCAAACCT
PMAIP1_BS1_Reverse	GCATCTCTTGGAAAACCAGAA
PMAIP1_BS2_Forward	TTCGGCGAAAACACACATT
PMAIP1_BS2_Reverse	GAAAATTGCCCAAGTTCACTT
PMAIP1_BS3_Forward	CTCGCCAAACATTATGCAAA
PMAIP1_BS3_Reverse	CGAGTGGATCGTTATCATATGG
PMAIP1_BS4_Forward	GACGACGTCCAGCGTTTG
PMAIP1_BS4_Reverse	GCCCCGAAATTACTTCCTTAC
PMAIP1_BS5_Forward	CACCGTGTGTAGTTGGCATC
PMAIP1_BS5_Reverse	AACCTCAGCCTCCAACTGG
PMAIP1_3'UTR_Forward	AGGCAGCTATTTTACCATCTGG
PMAIP1_3'UTR_Reverse	GTTTACTGCCACAGTATCAACTTTT

主論文: Oncogenesis. 2020 Feb 18;9(2):26.

公表済 doi: 10.1038/s41389-020-0205-4